F. J. Renk[1]
P. C. Wayner, Jr.

Department of Chemical and Environmental Engineering,
Rensselaer Polytechnic Institute,
Troy, N. Y. 12181

An Evaporating Ethanol Meniscus

Part I: Experimental Studies

The profile of an evaporating ethanol meniscus was measured as a function of the evaporative heat flux using interferometry. A measure of the evaporative heat flux was obtained using vapor deposited resistance thermometers. The meniscus profile was found to be stable and a function of the heat flux for the heat flux range of 0 − 1.36w/m of interline. These results were used in an analysis of capillary flow heat transfer in Part II.

Introduction

It is evident that evaporation and the resulting fluid flow in the vicinity of the triple interline (junction of solid-liquid-vapor) and the adjacent meniscus can control the change-of-phase heat transfer process occurring in various engineering devices such as heat pipes, boilers and grooved evaporators. It is likely that the study of heat transfer and fluid flow in a stationary evaporating meniscus will prove useful to understanding and improving these processes. However, limited experimental data are available for these regions because of the associated very small dimensions and the resulting very large gradients. The extended meniscus can be divided into three zones: (1) the immediate vicinity of the interline—the thin film region—where the thickness of the liquid can vary from a monolayer to approximately 5×10^{-8} m and where the fluid flow results from the pressure gradient produced in the liquid by the varying force of attraction between the liquid and solid (disjoining pressure), (2) the inner intrinsic meniscus region where the thickness range is approximately $(0.05 - 10) \times 10^{-6}$ m and where fluid flow resulting from very large pressure gradients due to curvature is possible, and (3) the outer intrinsic meniscus region where the thickness is greater than 10^{-5} m and where fluid flow resulting from small pressure gradients due to curvature is possible. Because of the large variation of the film thickness in the extended meniscus, it is currently necessary to study these regions independently. The objective of the experimental study described herein was to measure the inner intrinsic meniscus profile in the thickness range $(0.1 - 4) \times 10^{-6}$ m as a function of heat flux [1]. The optical technique of interferometry was used to obtain the meniscus profile and resistance thermometry was used to obtain the heat flux. The approximate location of the interline was also obtained. This experimental design was also used in a preliminary study which did not include an independent measurement of the heat flux and the interline location [2].

In Part II of this study [3], the measured heat flux was used in a model of the fluid flow field to obtain optimum agreement between the measured and predicted fringe locations. The resulting model equation was then used to obtain the curvature distribution, the heat flux distribution and the predicted interline location. The results of these coupled studies demonstrate that fluid flow in an evaporating meniscus results from a change in the meniscus profile which depends on the heat flux distribution. A previous experimental study of the outer meniscus region is in agreement with this conclusion [4].

Experimental Design and Procedure

A cross section of the test cell is presented in Fig. 1. A two-dimensional, horizontal meniscus was formed at the exit of the gap between the glass substrate (microscope slide) and the Teflon insert. The gap spacing was adjusted to 1.8×10^{-4} m and the liquid level was positioned at 6×10^{-3} m below the glass surface so that a stable, nonevaporating meniscus formed in which the pressure difference across the meniscus balanced the hydrostatic pressure drop at the start of a test run. The pressure was maintained slightly above atmospheric by adjusting the liquid storage levels. The glass substrate was cleaned in an ethanol vapor degreasing unit prior to installation in the test cell. Ethanol was also used as the test fluid because it wets glass very well. The dimensions of the glass substrate were 0.025 m × 0.076 m × 0.001 m.

Thin film nickel resistors—approximately 10^{-7} m thick, 1.27×10^{-4} m wide and 1.25×10^{-2} m long—with a resistance of approximately 500 ohms were vapor deposited on both sides of the glass substrate as shown in Fig. 2. Several of these on the upper surface were used to generate heat which was conducted through the glass to the meniscus region where evaporation occurred. The remainder were calibrated and used as resistance thermometers to measure the temperature distribution on the glass surface.[2] In addition, thermocouples were used to measure the temperature at various locations in the test cell. The substrate temperature distribution for four settings of the heater power input are presented in Fig. 3. The evaporating meniscus was stable during these tests and did not appear to vibrate. However, at significantly higher power settings a fluctuating meniscus was observed. The tests were conducted by first fixing the shape of the isothermal meniscus and then setting the power level so that evaporation occurred. The reported data represent the results of one continuous test run. No attempt was made to measure the maximum stable heat flux for the nonfluctuating case.

The test cell was mounted on a movable stage of a microscope so that the meniscus could be observed and photographed at 350× using monochromatic light with a wavelength of 5.89×10^{-7}m. Because of

[1] Present address: Westvaco Research Laboratory, Laurel, MD

Contributed by the Heat Transfer Division for publication in the JOURNAL OF HEAT TRANSFER. Manuscript received by the Heat Transfer Division March 27, 1978.

[2] A Keithley Model 520 nanowatt dissipation resistance bridge was used.

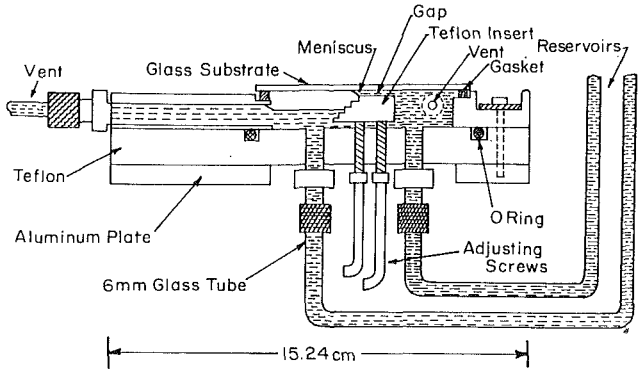

Fig. 1 Cross section of test cell (not drawn to scale)

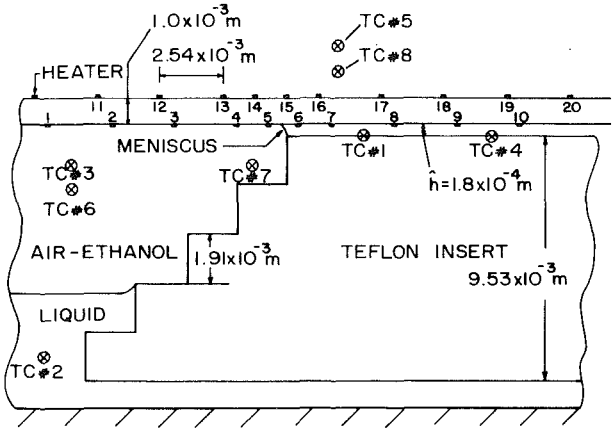

Fig. 2 Location of vapor deposited resistance thermometers

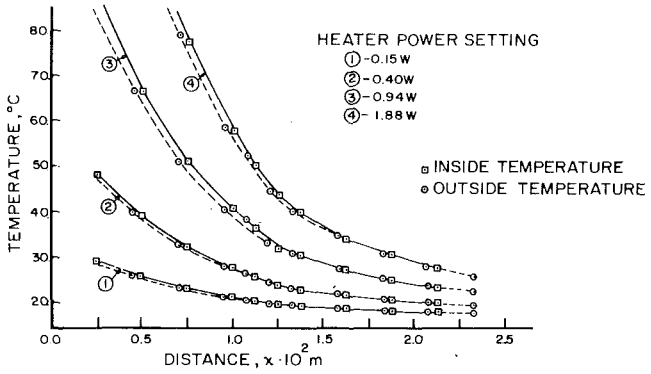

Fig. 3 Substrate temperature versus distance from heater

the significant difference between the refractive index of the glass, 1.5, and the ethanol liquid, 1.36, the interference patterns formed by the light waves reflected from the glass-liquid and liquid-vapor (ethanol-air mixture) boundaries were easily photographed for the various power settings. The photographic negatives were passed between a light source and a fiber optic probe connected to a photometer. The amount of transmitted light is an indication of the local film density. Using this densitometry method, the fringe locations were measured to an accuracy of approximately $\pm 10^{-7}$ m. The fringe number, No. 1 = first dark fringe, No. 2 = first light fringe, etc., is plotted versus the measured fringe location from the interline in Fig. 4 for the test runs. It is obvious that the fringes moved closer together as the heat flux was increased indicating a change in the meniscus shape due to evaporation.

In this experimental design, there is no change in the phase of lightwaves upon reflection at the boundaries because of the ever increasing refractive index. Therefore, the meniscus thickness profile, $h(x)$, can be related to the fringe location as follows:

$$\left.\begin{matrix}\text{minimum}\\ \text{intensity}\end{matrix}\right\} h = \frac{(2L+1)\,\lambda\,(\cos\theta)}{2n_\ell\,(1+\cos\theta)}, \quad L = 0, 1, 2\ldots \tag{1}$$

$$\left.\begin{matrix}\text{maximum}\\ \text{intensity}\end{matrix}\right\} h = \frac{L\lambda\,(\cos\theta)}{n_\ell\,(1+\cos\theta)}, \quad L = 0, 1, 2\ldots \tag{2}$$

where θ is the local meniscus slope. The meniscus thickness at the first fringe can be calculated using (1) if the slope is neglected:

$$h_1 = \lambda/4n_\ell \tag{3}$$

For an ethanol meniscus this gives a thickness of 1.08×10^{-7} m. Each succeeding fringe, minimum and maximum, represents a thickness increase of approximately this amount. Microscope slide roughness (Corning glass) was not examined explicitly. However, an evaluation of the uniformity of the fringes in the width and length direction did

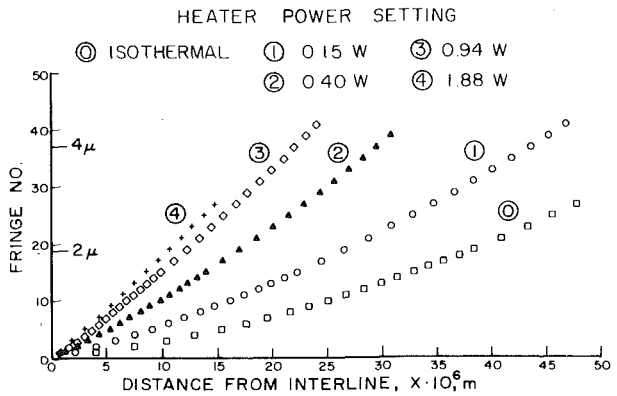

Fig. 4 Fringe number (No. 1 = first dark fringe, No. 2 = first light fringe, etc.) versus distance from interline, $X = x + |\hat{x}|$. ($x = 0$ at first fringe)

Nomenclature

H = latent heat of vaporization, $J \cdot kg^{-1}$
k = thermal conductivity of substrate, $Jm^{-1}\,s^{-1}\,K^{-1}$
N = fringe number, dimensionless
$\overline{Q}_e$ = nondimensional evaporative heat dissipation
Q^* = total evaporative heat dissipation per unit width, $w - m^{-1}$
$\overline{\overline{Q}}$ = nondimensional heat flow rate conducted in substrate
$\overline{T}$ = temperature, °C
h = local meniscus thickness, m
k = thermal conductivity of glass substrate
n_ℓ = refractive index of liquid, dimensionless
$\dot{n}$ = local volumetric flow per unit width, $m^3 \cdot s^{-1} \cdot m^{-1}$
$\dot{n}^*$ = total incoming volumetric flow per unit width, $m^3 \cdot s^{-1} \cdot m^{-1}$
t = thickness of substrate, m
x = coordinate along meniscus, m
w = width of glass substrate
γ = defined in equations (5) and (6)
$\overline{\theta}$ = nondimensional temperature
$\overline{\overline{\theta}}$ = nondimensional temperature averaged over width and thickness
θ = meniscus angle, radians
λ = wavelength of light, m
ξ = nondimensional coordinate in x-direction
ρ_ℓ = liquid density, $kg \cdot m^{-3}$

Superscripts

i = into meniscus region
j = out of meniscus region

not indicate the presence of a roughness effect. Although constructive interference occurs for small meniscus thicknesses, the location of the meniscus interline, if indeed a finite contact angle meniscus existed, was not sharply defined in our studies because of the relative intensities of the reflected light and the sensitivity of our equipment. Some information concerning the interline could be obtained but in most cases it was possible to determine only a right most bound for the interline location. That is, the point at which the presence of some liquid was detectable by observable interference. The measured value of this interline location is plotted versus the predicted value, from the model discussed in Part II, for the four power settings in Fig. 5. The interline location is given relative to the first fringe location which lies to the right of the interline. As expected, this distance decreased with an increase in the heat flux. In the nonevaporating case, a meniscus curvature of 1.6×10^{-1} m^{-1} was determined using interferometry versus an expected value of 2×10^{-3} m^{-1} based on hydrostatics. This difference is attributed primarily to insufficient accuracy in the measurement of the actual liquid level in the cell. This initial difference is not believed to effect the conclusions arrived at below because of the relatively large changes in meniscus shape on heating. Additional information concerning these experiments are available in [1].

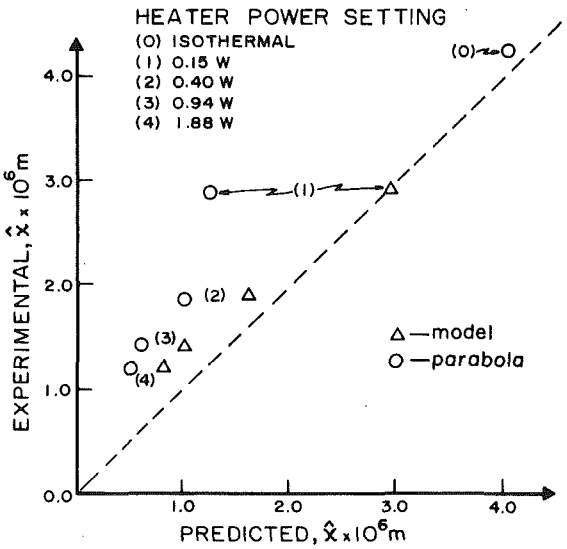

Fig. 5. Experimental versus predicted value of interline location relative to first fringe, $x = -\hat{x}$

Analysis of Temperature Data

The glass surface temperatures measured with the resistance thermometers are plotted in Fig. 3. Each measurement represents the surface temperature at a particular location averaged over one half of the width of the glass substrate (resistor length = 0.0125 m) and the width of the thin film resistor, 1×10^{-4} m. Using a two-dimensional analysis the substrate temperature was found to vary approximately 3 percent from its maximum value at the substrate centerline to its value at the edge of the resistance thermometer [1]. The precision of each temperature measurement was approximately ±0.1 °C. This was due to an uncertainty of ±0.05 ohms in measuring the resistance of the nickel thin films. Since we are concerned with heat flux rather than absolute temperature, the calibration error associated with the absolute temperature is of less importance. The temperature distribution, $\overline{T}(x)$, can be made nondimensional by defining

$$\xi = \frac{x}{w}; \quad \bar{\theta} = \frac{\overline{T} - T_\infty}{T_2 - T_\infty} \tag{4}$$

where T_∞ is the ambient temperature, $\overline{T}_2$ is the temperature measured by resistance thermometer No. 2 at that particular power input setting and w is the glass substrate width. As a result of this scaling, the data for all power input settings become nearly similar. In Fig. 6, the natural logarithm of the nondimensional temperature, ln $\bar{\theta}$, is plotted versus distance, ξ, for power setting No. 3, which is a typical case. Away from the evaporating meniscus region, the data indicate that the temperature can be assumed to be that of one-dimensional heat conduction in a thin slab with natural convection losses from the top surface. An analysis of conduction in the glass away from the meniscus region confirms this experimental result [1]. The data are well represented by the following equations

$$\bar{\bar{\theta}}^{(i)}(\xi) = \bar{\bar{\theta}}_0^{(i)} \exp(-\gamma^{(i)}\xi); \quad \xi < 0.3 \tag{5}$$

$$\bar{\bar{\theta}}^{(j)}(\xi) = \bar{\theta}_0^{(j)} \exp(-\gamma^{(j)}\xi); \quad \xi > 0.4 \tag{6}$$

where $\bar{\bar{\theta}}$ is the nondimensional temperature averaged over one half the substrate width and the thickness. The nondimensional heat flow rate, $\bar{\bar{Q}}(\xi) = -\gamma\bar{\bar{\theta}}$, can be obtained by differentiation of the one dimensional model equations (5) and (6). A measure of the heat removed by evaporation can be obtained by extending the one-dimensional model to the location of the meniscus interline. The line $\xi = 0.3$ corresponds to the location of resistance thermometer No. 4. The line $\xi = 0.4$ corresponds to the location of No. 6. Resistance thermometer No. 5 is located at $\xi = 0.36$. The temperature measured by sensor No. 5 is lowered by the proximity of the interline heat sink. Therefore, only the first four sensors were used to extrapolate the incoming heat flux to the meniscus interline. The heat flow rate out of the glass in the meniscus region which is predominately due to evaporation, $\overline{Q}_e$, is

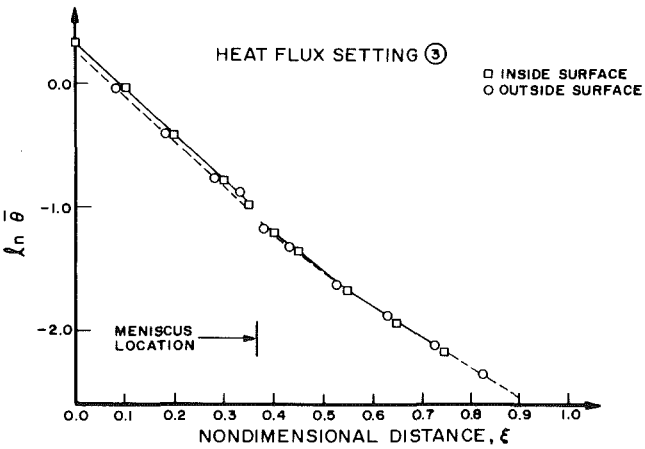

Fig. 6 Natural logarithm of the nondimensional temperature versus nondimensional distance from heater

equal to the difference between the incoming and outgoing heat flow rates in the glass

$$\overline{Q}_e = \overline{\bar{Q}}^{(i)} - \overline{\bar{Q}}^{(j)} \qquad \xi = \frac{\text{meniscus}}{\text{location}} \tag{7}$$

The actual evaporative heat loss from the glass due to evaporation per unit width can be calculated using

$$Q^* = \frac{kt}{w}(\overline{T}_2 - T_\infty)\overline{Q}_e \tag{8}$$

The above analysis demonstrates that the heat flux based on the interline length varied from zero to 1.36 w/m in our tests. This maximum level of heat flow can be averaged over the first 10^{-5} m to obtain an estimate of the average heat flux based on the area equal to 1.36×10^5 w/m^2. The results show that the ratio $Q_e/\overline{\bar{Q}}^{(i)}$ decreases from 0.31 to 0.22 as the power input setting is increased [1]. This indicates that substrate conduction limits the amount of heat delivered to the meniscus for evaporation. The incoming volumetric flow rate which must be evaporated per unit width to account for this heat flux can be calculated using

$$\dot{m}^* = Q^*/\rho_\ell H \tag{9}$$

where ρ_ℓ is the density of the liquid and H is the latent heat of vaporization. The results obtained for all power input settings are given in Table 1.

Table 1

Heat Flux Setting	1	2	3	4
$\bar{\bar{\theta}}_0^{(i)}$	1.42	1.42	1.43	1.44
$\bar{\bar{\theta}}_0^{(j)}$ ($\xi = 0.4$)	0.31	0.31	0.30	0.29
$\gamma^{(i)}$	3.75	3.75	3.80	3.95
$\gamma^{(j)}$	2.72	2.96	3.10	3.20
ξ meniscus	0.360	0.362	0.365	0.368
$\bar{\bar{Q}}^{(i)}$ (ξ meniscus)	1.38	1.37	1.36	1.33
$\bar{\bar{Q}}^{(j)}$ (ξ meniscus)	0.94	1.03	1.04	1.03
$\bar{Q}_e$	0.44	0.34	0.32	0.30
$\bar{Q}_e/\bar{\bar{Q}}^{(i)}$ (ξ meniscus)	0.31	0.25	0.24	0.22
Q^* [w/m]	0.18	0.37	0.79	1.36
$\dot{n}^*$ [$m^3/m - s \times 10^{10}$]	2.60	5.35	12.74	20.48

The error in the determination of $\bar{Q}_e$ can be obtained from estimates of the error in determining the one dimensional heat flux into and away from the meniscus region. The relative error for the nondimensional heat flux can be calculated as

$$\frac{\Delta\bar{Q}}{\bar{Q}} = \frac{\Delta\gamma}{\gamma} + \frac{\Delta\theta_0}{\bar{\bar{\theta}}_0} \tag{10}$$

The estimates for these quantities are $\Delta\gamma = \pm 0.025$ and $\Delta\bar{\bar{\theta}}_0 = \pm 0.05$. The uncertainty in determining the interline location is insignificant in this case. Using equation (10) for both the incoming and outgoing heat flux, an error estimate of 13 percent for the evaporative heat flux is obtained for the worst case.

Discussion and Conclusions

The experimental results presented above significantly increase the available data concerning the steady-state evaporating meniscus. In order to complete the study, a mathematical model is now needed to relate the observed change in the meniscus profile to the evaporative heat flux obtained from the temperature measurements. The model must relate the shape of the evaporating meniscus to the pressure gradient needed to supply the volumetric flow rate to maintain steady-state evaporation. The solution to this involved problem is discussed in Part II [3]. Briefly, we can say that the measured fringe locations for all heat flux settings were analyzed using the measured heat flux in a nonlinear parameter estimation technique. By assuming a mathematical model for the meniscus profile with adjustable parameters, the fringe location data were used to select those parameters which yielded the best agreement between the measured and predicted fringe location in the least squares sense. The results of this analysis demonstrated that a model which included fluid flow resulting from a curvature gradient represented the data better than a constant curvature model.

Using only the experimental results, we can state that:

1 the average evaporative heat flux in an evaporating meniscus has been measured for the range 0–1.36 w/m of interline using resistance thermometers vapor deposited on the galss substarte; and

2 the profile of an evaporating meniscus has been measured in the thickness range $(0.1–4) \times 10^{-6}$ m using the optical technique of interferometry.

These measurements lead to the conclusion that the evaporating meniscus profile is stable and that it is a function of the evaporative heat flux.

Acknowledgment

The financial support received through National Science Foundation Grants GK-43116 and ENG 76-01608 are gratefully acknowledged.

References

1 Renk, F. J., "Analytical and Experimental Investigation of an Evaporating Meniscus" Ph.D. Dissertation, Rensselaer Polytechnic Institute, Troy, N. Y., 1977.

2 Renk, F. and Wayner, P. C., Jr., "The Measurement of Fluid Flow and Heat Transfer in an Evaporating Meniscus," *Proceedings of the Fifth International Heat Transfer Conference,* Vol. 5, 1974, pp. 252–256.

3 Renk, F. and Wayner, P. C., Jr., "An Evaporating Ethanol Meniscus: Part II, Analytical Studies," ASME JOURNAL OF HEAT TRANSFER, Vol. 101, No. 1, 1979, pp. 59–62.

4 Preiss, G. and Wayner, P. C., Jr., "Evaporation from a Capillary Tube," ASME JOURNAL OF HEAT TRANSFER, May 1976, pp. 178–181.